

**REPORT DOCUMENTATION PAGE****Form Approved**  
**OMB No. 0704-0188**

Public reporting burden for this collection of information is estimated to average 1 hour per response, including the time for reviewing instructions, searching data sources, gathering and maintaining the data needed, and completing and reviewing the collection of information. Send comments regarding this burden estimate or any other aspect of this collection of information, including suggestions for reducing this burden to Washington Headquarters Service, Directorate for Information Operations and Reports, 1215 Jefferson Davis Highway, Suite 1204, Arlington, VA 22202-4302, and to the Office of Management and Budget, Paperwork Reduction Project (0704-0188) Washington, DC 20503.

**PLEASE DO NOT RETURN YOUR FORM TO THE ABOVE ADDRESS.**

<b>1. REPORT DATE (DD-MM-YYYY)</b> 21-Jun-06		<b>2. REPORT TYPE</b> Final		<b>3. DATES COVERED (From - To)</b> Jan 05 - Apr 06	
<b>4. TITLE AND SUBTITLE</b> Oxide Films RF Applications				<b>5a. CONTRACT NUMBER</b> N00014-05-1-0152	
				<b>5b. GRANT NUMBER</b> 06PR04151-00	
				<b>5c. PROGRAM ELEMENT NUMBER</b>	
<b>6. AUTHOR(S)</b> SKOWRONSKI, Marek				<b>5d. PROJECT NUMBER</b>	
				<b>5e. TASK NUMBER</b>	
				<b>5f. WORK UNIT NUMBER</b>	
<b>7. PERFORMING ORGANIZATION NAME(S) AND ADDRESS(ES)</b> Carnegie Mellon University Office of Sponsored Research 5000 Forbes Avenue Pittsburgh PA 15213				<b>8. PERFORMING ORGANIZATION REPORT NUMBER</b>	
<b>9. SPONSORING/MONITORING AGENCY NAME(S) AND ADDRESS(ES)</b> Office of Naval Research Regional Office Chicago 230 South Dearborn, Room 380 Chicago IL 60604-1595				<b>10. SPONSOR/MONITOR'S ACRONYM(S)</b> N62880	
				<b>11. SPONSORING/MONITORING AGENCY REPORT NUMBER</b> ONR 245	
<b>12. DISTRIBUTION AVAILABILITY STATEMENT</b>  <b>DISTRIBUTION STATEMENT A</b> Approved for Public Release Distribution Unlimited					
<b>13. SUPPLEMENTARY NOTES</b>					
<b>14. ABSTRACT</b>  TiO <sub>2</sub> films were grown using a reactive molecular beam epitaxy system equipped with high-temperature effusion cell for Ti and ozone. The growth mode, characterized in-situ by reflection high-energy electron diffraction (RHEED), as well as the phase assemblage, structural quality, and surface morphology, characterized ex-situ by X-ray diffraction and atomic force microscopy (AFM), depended on the choice of substrate, growth temperature, and ozone flux. Films deposited on (100) surfaces of SrTiO <sub>3</sub> , (La <sub>0.27</sub> Sr <sub>0.73</sub> )(Al <sub>0.65</sub> Ta <sub>0.35</sub> )O <sub>3</sub> , and LaAlO <sub>3</sub> grew as (001)-oriented anatase. Both RHEED and AFM indicated that smoother surfaces were observed for those grown at higher ozone fluxes.					
<b>15. SUBJECT TERMS</b>					
<b>16. SECURITY CLASSIFICATION OF:</b>			<b>17. LIMITATION OF ABSTRACT</b>	<b>18. NUMBER OF PAGES</b>	<b>19a. NAME OF RESPONSIBLE PERSON</b>
a. REPORT	b. ABSTRACT	c. THIS PAGE			<b>19b. TELEPHONE NUMBER (Include area code)</b>

## **Final Technical Project Report**

Title: Oxide Films RF applications  
University: Carnegie Mellon University  
PIs: M. Skowronski & P. Salvador  
Agency: Office of Naval Research  
Award number: N00014-05-1-0152  
Performance period: 01/01/05-12/31/05  
Total award: \$200,000

**DISTRIBUTION STATEMENT A**  
Approved for Public Release  
Distribution Unlimited

**20060710062**

The overall target for the project is optimization of tenability / dielectric loss ratio in oxide thin films. The targeted material systems are  $\text{Ba}_x\text{Sr}_{1-x}\text{TiO}_3$  alloys and digital alloys, specifically acentric superlattices. Project had four major tasks during the last year. These are listed and discussed in detail below.

## **1. Growth of high quality $\text{TiO}_2$ by Molecular Beam Epitaxy**

The critical issues in deposition of BSTO alloys is control of stoichiometry i.e. (Ba+Sr)/Ti ratio, oxygen stoichiometry, and structural quality of the film. The first stepping stone toward this goal was controlled deposition of high quality of  $\text{TiO}_2$  by MBE. This task required calibration of Ti and O fluxes, monitoring of substrate temperature and growth initiation procedures, and film growth mode by RHHED. Besides potential benefits for goals of the project, there is a wide technological interest in  $\text{TiO}_2$  because it has interesting physical and chemical properties, which make it appealing for optical, dielectric, electrochemical, and photocatalytic applications.  $\text{TiO}_2$  is also of scientific interest since it has polymorphic structures (anatase, rutile, and brookite) that exhibit different stabilities and properties. Certain applications, such as integrated dielectrics or photoelectrochemical cells, require thin films of  $\text{TiO}_2$  that exhibit a specific crystal structure, orientation, and/or morphology.

The growth is of interest to RF project for three reasons. One is that rutile has interesting dielectric properties. Another is that the (001) plane of anatase  $\text{TiO}_2$  is one of the two main layers stacked along the (100) direction in cubic  $\text{Ba}_{1-x}\text{Sr}_x\text{TiO}_3$ — the other being the (100) plane of rock-salt SrO. Hence, to grow films using atomic layer-by-layer molecular beam epitaxy, it is essential to understand the growth of  $\text{TiO}_2$  in MBE. There exists a considerable gap in the archival literature concerning the growth of  $\text{TiO}_2$  over a range of process parameters. The final reason is that, in non-stoichiometric films, local regions of  $\text{TiO}_2$  inclusions or  $\text{TiO}_2$  intergrowths may develop in otherwise perfect  $\text{Ba}_{1-x}\text{Sr}_x\text{TiO}_3$ . As such, we investigated the MBE growth of  $\text{TiO}_2$ .

A summary of our findings are as follows.  $\text{TiO}_2$  films were grown using a reactive molecular beam epitaxy system equipped with high-temperature effusion cells as sources for Ti and an ozone distillation system as a source for oxygen. The growth mode, characterized *in-situ* by reflection high-energy electron diffraction (RHEED), as well as the phase assemblage, structural quality, and surface morphology, characterized *ex-situ* by X-ray diffraction and atomic force microscopy (AFM), depended on the choice of substrate, growth temperature, and ozone flux. Films deposited on (100) surfaces of  $\text{SrTiO}_3$ ,  $(\text{La}_{0.27}\text{Sr}_{0.73})(\text{Al}_{0.65}\text{Ta}_{0.35})\text{O}_3$ , and  $\text{LaAlO}_3$  grew as (001)-oriented anatase. Both RHEED and AFM indicated that smoother surfaces were observed for those grown at higher ozone fluxes. Moreover, while RHEED patterns indicated that anatase films grown at higher temperatures were smoother, AFM images showed presence of large inclusions in these films.

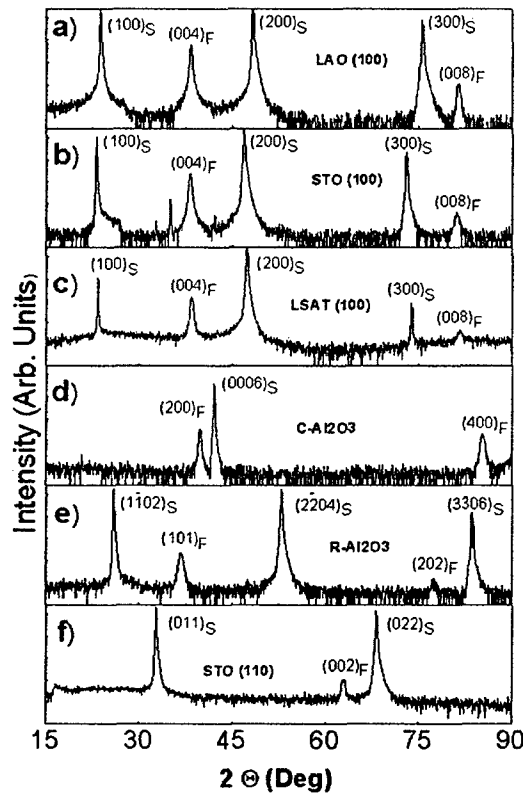


**Figure 1**  $\theta$ - $2\theta$  scans of  $\text{TiO}_2$  films on (a)  $\text{LaAlO}_3$  (100), (b)  $\text{SrTiO}_3$  (100), (c) LSAT (100), (d,e)  $\text{Al}_2\text{O}_3$  (0001) and (1-102), and (f)  $\text{SrTiO}_3$  (110) substrates.

The XRD spectra of  $\text{TiO}_2$  films deposited on 6 substrates at  $750^\circ\text{C}$  are shown in Figure 1. These XRD patterns reveal that highly (001)-oriented anatase films grew on  $\text{SrTiO}_3$  (100), LSAT (100), and  $\text{LaAlO}_3$  (100) substrates. In fact, similar XRD results were observed by us for anatase films deposited over a wide range of conditions ( $450^\circ < T_d < 750^\circ\text{C}$  and  $0.25 < \text{flux O}_3 < 2.00$ ).  $\phi$ -scans showed that these films were all epitaxial and all had the same relationship:  $(001)_{\text{TiO}_2} \parallel (100)_{\text{Subs}} ; [010]_{\text{TiO}_2} \parallel [010]_{\text{Subs}}$ . The full widths at half maximum (FWHM) of the rocking curve on the anatase (004) peaks were largest for the films on  $\text{SrTiO}_3(100)$  ( $\approx 0.7^\circ$ ), intermediate on LSAT ( $\approx 0.1^\circ$ ), and lowest ( $\approx 0.03^\circ$ ) on  $\text{LaAlO}_3(100)$ . The FWHM for the substrates themselves were all  $\approx 0.02^\circ$  under our diffraction conditions, indicating that the films on  $\text{LaAlO}_3$  substrates were of superior crystalline quality to the other two films, in spite of the inherent twinning in the  $\text{LaAlO}_3$  substrate. These diffraction observations are similar in nature to those observed in other reports using other deposition methods [11,16] and using MBE deposition [8], although no other reports exist on MBE growth of  $\text{TiO}_2$  films on the LSAT(100) surface. It should be noted that epitaxial rutile  $\text{TiO}_2$  films were observed for C-cut and R-cut sapphire, as well as (110)-STO.

Figure 2 shows RHEED images, taken along the [100] azimuth, of anatase films grown at  $750^\circ\text{C}$  using a Ti-cell temperature of  $1550^\circ\text{C}$  and an ozone flux of 1 sccm on (a)  $\text{SrTiO}_3(100)$ , (b) LSAT(100), and (c)  $\text{LaAlO}_3(100)$ . All RHEED patterns were consistent with anatase(001) growth and exhibited a characteristic four-fold reconstruction of this anatase surface. Figure 1 shows that the RHEED patterns for the films grown on  $\text{LaAlO}_3$  are sharper and Kikuchi lines are more clearly evident than on  $\text{SrTiO}_3$  or LSAT, indicating better surface morphology and higher crystallinity for the films on  $\text{LaAlO}_3$ . This is likely because of the excellent lattice match between anatase and  $\text{LaAlO}_3(100)$  ( $f = 0.3\%$ ).

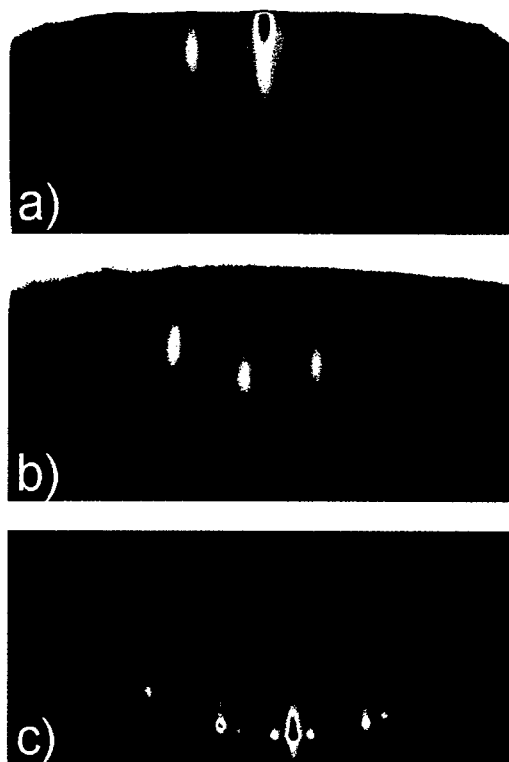


**Figure 2** RHEED image taken along the [100] azimuth at the end of film growth for  $\text{TiO}_2$  films deposited on (a)  $\text{SrTiO}_3$  (100), (b) LSAT (100), and (c)  $\text{LaAlO}_3$  (100).

RHEED intensity oscillations were observed consistently for the films grown on  $\text{LaAlO}_3$  substrates. Thicknesses of films were determined using X-ray reflectance. Combining this with the RHEED oscillations, we calculated that one RHEED intensity oscillation corresponded to the growth of  $\approx 4.5 \text{ \AA}$  of anatase; that value is very close to a bilayer of anatase ( $\approx 4.75 \text{ \AA}$ ), in agreement with previous reports. Similar behavior (meaning growth via bilayer units) was obtained for the films grown with different Ti cell temperatures (i.e., growth rates), substrate temperatures, and ozone flux. The absence of RHEED oscillations for films grown on  $\text{SrTiO}_3$  and LSAT is reflective of the more diffuse nature of the diffraction patterns and an increase in the spottiness of the patterns, indicating that those surfaces are rougher compared to films on  $\text{LaAlO}_3$ .

To better understand surface morphologies, films were studied *ex-situ* with AFM. Two types of features are observed in the AFM images: a uniform grayish contrast that represents the matrix phase (and the major surface feature) and significantly brighter

spots that stand out from the uniform contrast and represent inclusions in the films. The grayscale changes in the uniform background decrease on going from  $\text{SrTiO}_3$  to LSAT to  $\text{LaAlO}_3$ , indicating a flatter surface of the matrix anatase. The overall grayscale was similar, however, between all the images because both LSAT and LAO exhibit bright white features indicative of large protrusions on the film surface.

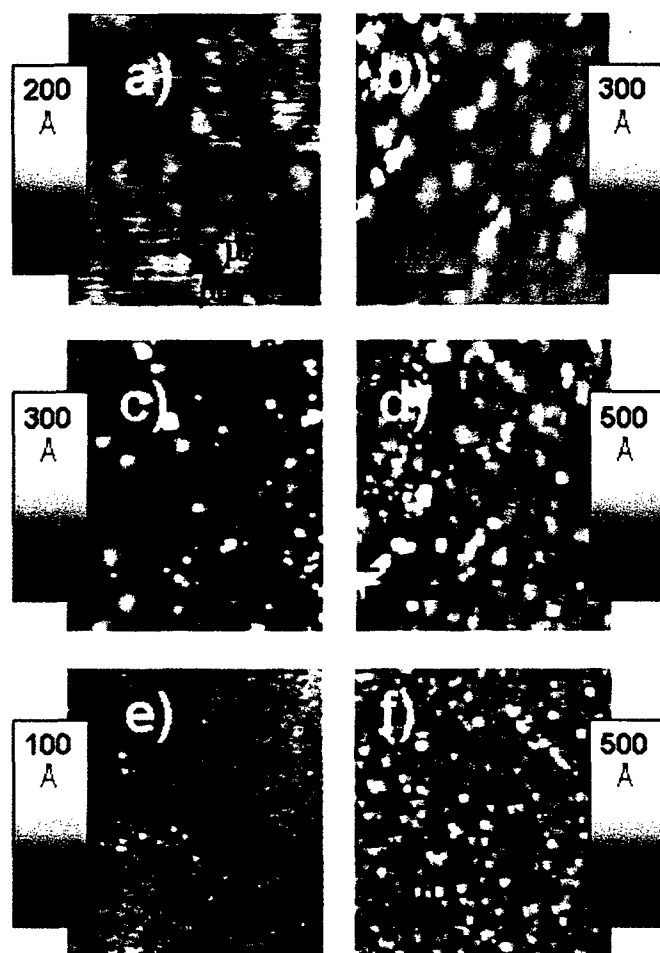


**Figure 3** (a)-(c) are AFM images of  $\text{TiO}_2$  films grown at  $750^\circ\text{C}$  using a Ti source temperature of  $1550^\circ\text{C}$  and an ozone flux of 1 sccm on (a)  $\text{SrTiO}_3(100)$ ; (b)  $\text{LSAT}(100)$ ; and on  $\text{LaAlO}_3(100)$ ; (d)-(f) are AFM images of  $\text{TiO}_2$  films grown on  $\text{LaAlO}_3(100)$  using a Ti source temperature of  $1550^\circ\text{C}$  at (d)  $750^\circ\text{C}$ , 0.25 sccm  $\text{O}_3$ ; (e)  $550^\circ\text{C}$ , 1.00 sccm  $\text{O}_3$ ; and (f)  $550^\circ\text{C}$ , 0.25 sccm  $\text{O}_3$ .

It should be pointed out that under the growth conditions investigated, temperature seemed to play the largest role on inclusion formation; substrate choice, ozone flux, and Ti-cell temperature played secondary roles, if any. Interestingly, the inclusions did not

appear to affect either the RHEED pattern or the XRD pattern in an obvious manner. Convergent beam electron microscopy experiments (discussed in the next section) indicated that these objects are rutile inclusions that have coherent interfaces with the anatase matrix and protrude out from the flat surface of the anatase matrix. Nevertheless, it should be noted that no rutile inclusions are observed in pure  $\text{TiO}_2$  films deposited using pulsed laser deposition on  $\text{LaAlO}_3(100)$  substrates at  $T=750^\circ\text{C}$  in elevated pressures of pure oxygen ( $P \approx 200\text{ mTorr O}_2$ ). Further work is required to understand the thermodynamics and kinetics of the nucleation and growth of these rutile inclusions during thin film deposition.

## 2. Structural characterization of oxide films

Electron microscopy was carried out on both substrates and films to better understand their dislocation density and phase distribution. Figure 4 is a bright field TEM of the STO substrate grown by Verneuil method. The dark lines correspond to dislocations, their density was estimated at  $4.3 \times 10^8/\text{cm}^2$ . In the future, we will routinely compare the number and type of dislocations that form in perovskite films to those present in the perovskite substrates.

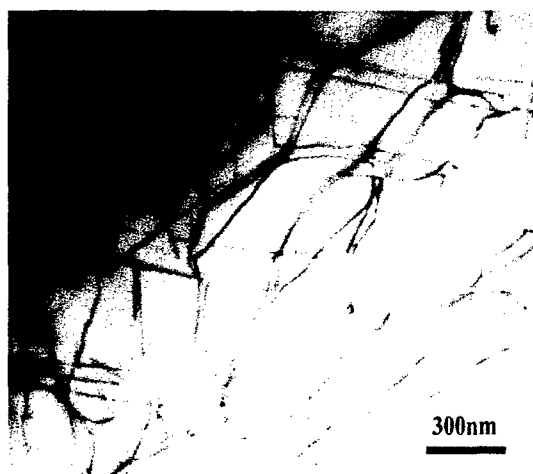


**Figure 4** Bright field image of the  $\text{SrTiO}_3$  substrate. The average dislocation density in this STO substrate is about  $4.3 \times 10^8/\text{cm}^2$

As an indication of how TEM experiments complement the RHEED / XRD / AFM results discussed in previous section, we present our results on MBE grown  $\text{TiO}_2$  films under conditions that lead to large inclusions observed by AFM.

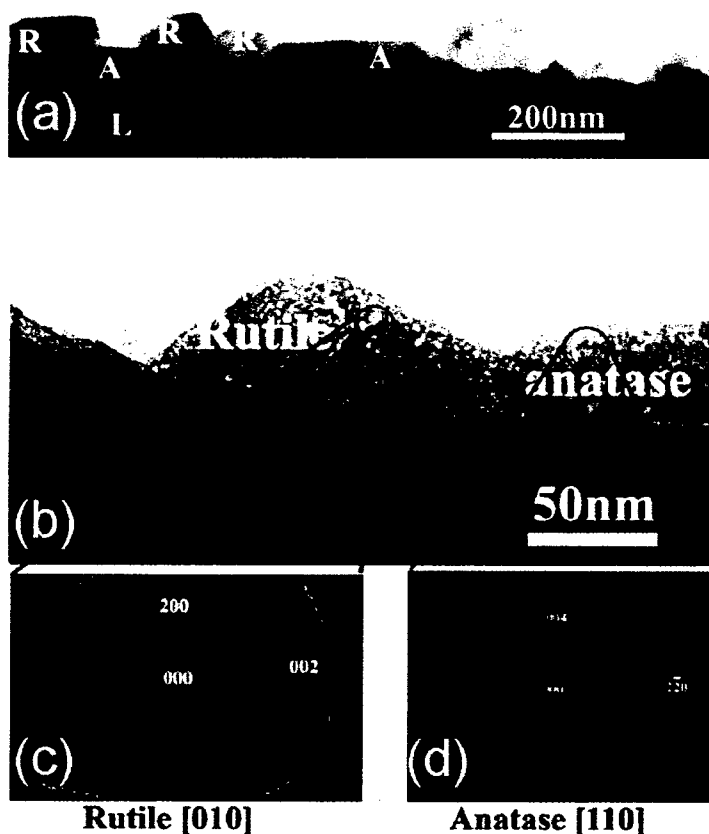


**Figure 5** (a) and (b), bright field TEM images of MBE-grown  $\text{TiO}_2$  films on  $\text{LaAlO}_3$ . Regions marked R are rutile inclusions in the anatase matrix marked A. (c) and (d) Convergent Beam Electron Diffraction images from the two regions, (c) from rutile and (d) from anatase.

Figure 4(a) and (b) show two cross sectional HREM images that demonstrate the inclusions do indeed protrude from the surface of a flat matrix film. The Convergent Beam Electron Diffraction images given in Figure 4(c) and (d) illustrate that the matrix phase is anatase and the inclusions are rutile. High resolution images show that the matrix phase and inclusions are coherent with one another. Interestingly, PLD-deposited films do not exhibit these inclusions, even at similar deposition temperatures.

### 3. Hybrid oxide growth system design and installation

In parallel with setting up the MBE chamber at PennState EOC and running growth experiments, a second system was designed and set up at Carnegie Mellon University. The funding was provided from internal sources. The chamber is a hybrid growth system capable of operating in two modes: Pulsed Laser Deposition in UHV environment and full Molecular Beam Epitaxy mode using Knudsen cells as metal sources. A schematic drawing of the chamber is shown in Fig. 6.

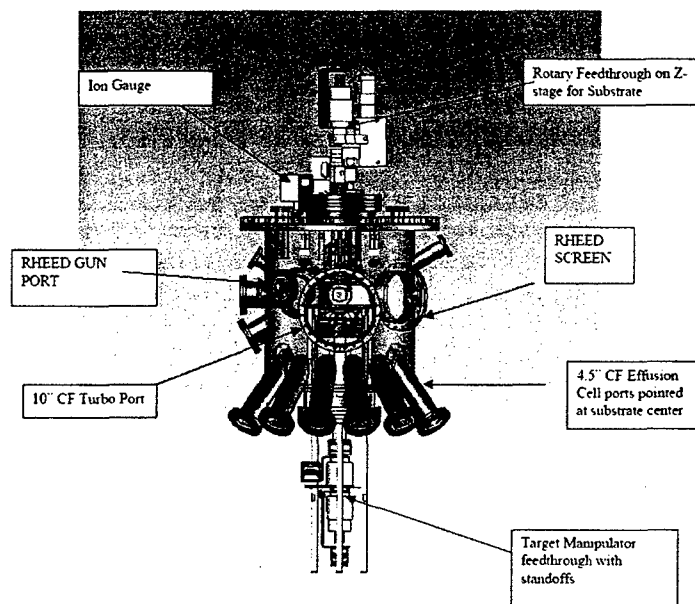


**Figure 6** Schematic drawing of the deposition chamber installed at CMU and being used for deposition of oxide films.

At this point, the chamber operates as a UHV PLD system using the excimer laser as the excitation source. The chamber has ports to accommodate activated oxygen source (either RF plasma or ozone). The ozone source was already purchased and is being fitted into the chamber.

In the future, we are planning to add RHEED for in situ monitoring of the growth mode and K-cells for precise control of atomic fluxes at critical points in the growth sequence such as interface control.

#### **4. MBE of layered $(\text{SrO})_m(\text{TiO}_2)_n$ structures**

We have begun the deposition of SrO layers (as the component of barium-strontium-titanium oxide structures, and this has been successful. Single layers of rock salt SrO films were grown using similar conditions to  $\text{TiO}_2$  films growth. The growth is cube-on-cube-epitaxy on STO, LAO, and  $\text{TiO}_2$ . This work is preliminary and will not be discussed in great detail here. Films of  $\text{SrTiO}_3$  ( $m=1$ ,  $b=1$ ) and  $\text{Sr}_2\text{TiO}_4$  ( $m=2$ ,  $n=1$ ) have also been grown. XRD patterns correspond to c-axis growth of the perovskite and Ruddlesden-Popper phase, respectively. By combining RHEED oscillations, X-ray reflectometry, and RBS data (performed at Cornell University), we have optimized the growth rate to achieve stoichiometric monolayer coverage within  $\approx 1\%$  of the targeted stoichiometry. This work sets up the proposed work for the forthcoming period, Period 3. Importantly, we have succeeded in growing  $\text{SrTiO}_3$  and  $\text{Sr}_2\text{TiO}_4$  phases using MBE. Also, phases with higher strontium content were synthesized (pure SrO and  $\text{Sr}_3\text{TiO}_5$ ) and their X-ray patterns were recorded. However, such films were found to be unstable relative to decomposition in air. This is an important step towards understanding the complex phases and defect chemistry that might occur in dielectric films.